Physicochem. Probl. Miner. Process., 62(5), 2026, 237604

http://www.journalssystem.com/ppmp

Physicochemical Problems of Mineral Processing

ISSN 1643-1049

Gas dispersion characteristics of the Concorde Cell™

Berivan Tunç [1], Toni Mattsson [1], Alejandro Yáñez [1], Rodrigo Grau [1], Gülay Bulut [2]

[1] Metso, Finland

[2] Istanbul Technical University, Mining Faculty, Mineral Processing Department, Türkiye

Corresponding author: berivan.tunc@metso.com (Berivan Tunç)

Abstract: The flotation of fine and ultrafine particles has become increasingly important as ore grades decline and more complex deposits are processed. Their recovery is limited by low collision efficiency, which is strongly affected by particle and bubble size. Smaller bubbles increase collision probability and interfacial area, making gas dispersion a key descriptor of flotation performance. The main gas-dispersion parameters are bubble size, superficial gas velocity, gas hold-up and bubble surface area flux, the latter being commonly linked to flotation kinetics. The Concorde Cell™ is a high-intensity pneumatic flotation device operated under high shear conditions, where fine bubble generation is used to promote particle–bubble interactions. In this work, gas-dispersion characteristics of the Concorde Cell were examined at laboratory, pilot and industrial scales under controlled air–water conditions. The measurements covered a range of superficial gas velocities and operating conditions, with emphasis on bubble size distribution and gas hold-up. The measured gas-dispersion parameters followed comparable trends across scale. The pilot and industrial data showed close correspondence over the common operating range, while the industrial unit extended the measurements to higher gas hold-up and bubble surface area flux. The preservation of the d_{32} – J_g and S_b – J_g trends from laboratory to industrial scale supports the scale-up of the pulp-zone gas-dispersion conditions over the investigated operating range. The experiments were conducted under two-phase air–water conditions at frother concentrations above the critical coalescence concentration (CCC); therefore, the effects of solids, particle loading, and froth transport require further investigation.

Keywords: Concorde Cell, fine ultrafine flotation, gas dispersion, scale-up, bubble size

1. Introduction

Flotation performance is governed by the interaction of three key parameters: chemistry, ore, and machine (Klimpel, 1984). In recent years, the increasing demand for mineral resources has led to the treatment of more complex ore bodies with lower head grades (Calvo and Valero, 2022). Effective processing of fine and ultrafine particles has therefore become increasingly important. These particles present several inherent challenges due to their physical and chemical properties, including high surface area, low momentum, small mass, and elevated surface energy. As a result, they are more susceptible to rapid oxidation, reduced energy for bubble attachment, higher reagent consumption, and increased entrainment (Farrokhpay et al., 2021; Pease et al., 2006).

The successful bubble–particle capture process is controlled by the efficiency of collision, attachment, and stability (Dai et al., 1999). For fine particles, once attachment occurs, detachment is unlikely because the adhesive forces associated with surface tension dominate over centrifugal forces, which decrease more rapidly with particle size (Jameson, 2010). Thus, improving collision efficiency becomes a primary focus when aiming to enhance the flotation rate of fine and ultrafine particles (Schubert, 2008). Collision efficiency is strongly influenced by particle and bubble size, varying with the square of particle size and inversely with the square of bubble size (Yoon and Luttrell, 1989). This relationship supports observations that smaller bubbles, including micro- and nanobubbles, can significantly improve the recovery of fine particles (Ahmadi et al., 2014).

DOI: 10.37190/ppmp/237604

Bubble size reduction is achieved through mechanical or physicochemical means (Miettinen et al., 2010). Among mechanical approaches, cell design and hydrodynamic conditions, including flow regime, mixing intensity, solids suspension, gas dispersion, and bubble–particle interaction, influence flotation performance (Finch et al., 2000). Gas dispersion is a key parameter for characterizing flotation hydrodynamics and includes bubble size (d_{32}), superficial gas velocity (J_g), gas hold-up (ε_g), and bubble surface area flux ($S_b = 6J_g/d_{32}$) (Grau & Heiskanen, 2003). Bubble surface area flux is commonly used to relate gas dispersion to flotation kinetics (Gorain et al., 1997).

Despite research on gas dispersion in flotation systems, the effect of scale on gas dispersion properties from laboratory and pilot units to industrial operations remains a key aspect of flotation design (Saeed et al., 2022; Burstein and Filippov, 2010). Equipment geometry, flow regime, and operating conditions affect bubble size distribution, gas hold-up, and overall dispersion characteristics (Gorain et al., 1997). Reliable flotation scale-up therefore requires understanding how these parameters develop across scale.

This requirement is particularly relevant for high-intensity flotation technologies such as the Concorde Cell™, where gas dispersion controls bubble–particle contacting in the pulp zone. The Concorde Cell is a pneumatic flotation device operated under high shear conditions and designed to generate fine bubbles for fine and ultrafine particle flotation (Yáñez et al., 2024).

Gas-dispersion characteristics are commonly investigated under controlled air–water (two-phase) conditions before evaluation in flotation systems containing solids. The use of a two-phase system allows the effects of operating variables on bubble size distribution, J_g, and gas hold-up to be examined independently of particle loading and froth transport, and has been widely adopted for gas-dispersion characterization of flotation equipment (Gomez and Finch, 2007).

In the present study, J_g, bubble size distribution, and gas hold-up were examined in air–water two-phase systems; frothers were used to control and reduce the coalescence of air bubbles at laboratory, pilot, and industrial scales.

2. Materials and methods

Gas dispersion measurements were carried out in fully automated Concorde Cell units at laboratory, pilot, and industrial scales, equipped with an HMI-based control system for real-time monitoring of measurements and control of operating variables. The units were operated over a range of J_g, jet velocity, and pressure conditions. Main parameters are shown in Table 1.

Table 1. Main parameters of the cells

Concorde Cell ™ Model	Pilot Scale	Lab Scale	Industrial Scale
Tank volume, m^3	0.08	0.02	16.6
Feed flowrate, m^3/h	3.5	0.48	350
Air to pulp ratio	0.1 to 1.3	0.1 to 1.3	0.1 to 1.3
Blast tube diameter	2.5x	* 1x	25x

* × relative to the laboratory-scale Blast Tube diameter.

The Concorde Cell Lab Unit consists of flotation cell with a volume of 20 dm^3 and DN20 Blast Tube. In the lab-scale flotation, the pumped feed flow rate was maintained at 8 dm^3/min. In the Concorde Cell lab, 100% of the tailings are recycled back into the feed of the cell. Concorde Cell Pilot (80 dm^3 pilot-scale unit) continuous pilot-scale tests were performed to evaluate process stability and scalability of the technology under optimized test work conditions. In the pilot-scale flotation, the pumped feed flow rate was maintained at 52 dm^3/min. Concorde Industrial Unit equipped with a single Blast Tube was commissioned at Kevitsa mine in January 2025. At the laboratory scale, bubble size distribution, J_g, and gas hold-up were measured using the Pixact bubble sizing system and software (Pixact, 2026). At the pilot and industrial scales, bubble size distribution and J_g were measured using the same Pixact software coupled with a McGill viewing chamber, following the method of Hernandez-Aguilar et al. (2002). Gas hold-up at the pilot and industrial scales was measured using a dedicated sampling probe consisting of a vertical cylinder fitted with pneumatic valves at the top and bottom. The probe was immersed into

the pulp phase, allowed to fill with aerated slurry, and after a while isolated to determine the gas hold-up from the collected sample volume (Power et al., 2000; Schwarz and Alexander, 2006) (Fig. 1).

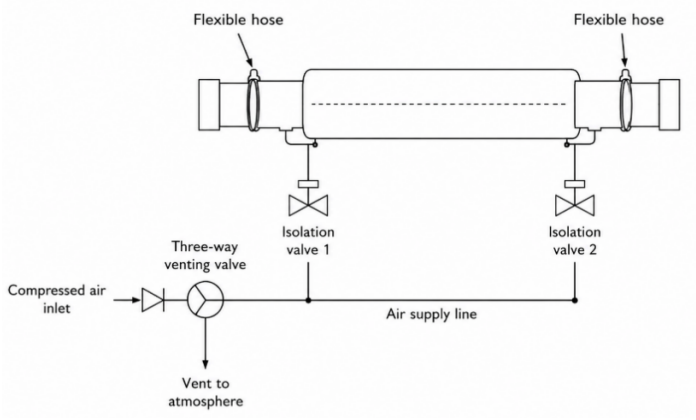

Fig. 1. Demonstration of gas hold-up measurement probe

For each operating condition, more than 150,000 bubbles were analysed to obtain a representative bubble size distribution. Three repeated bubble-size measurements were performed for a representative operating condition, and the standard deviation of the resulting, d_{32} ,values was calculated to assess measurement repeatability.

All tests were conducted in two-phase air-water systems. Tap water was used in the laboratory and pilot units, whereas process water was used in the industrial unit. A water-soluble glycol-ether-based frother (Nas Froth 240) was used for pilot and industrial unit measurements, whereas an alcohol-based (MIBC) frother was used for the lab-scale unit. MIBC was used at a concentration of 15 ppm. For Nas Froth 240, the concentration was initially set at 8 ppm and progressively increased to approximately 15 ppm while monitoring the bubble size. Frother addition continued until three consecutive bubble-size measurements showed no further measurable reduction with increasing frother concentration, indicating that the selected concentration was above the critical coalescence concentration (CCC) under the conditions of the present experiments.

Before each test series, water was pumped through the Concorde Blast Tube using a centrifugal pump until the liquid level reached the cell lip. Air was then introduced into the system. The frother was added incrementally, and bubble size was determined after each addition. Frother addition was continued until no further decrease in bubble size was observed, indicating that the frother concentration was above the critical coalescence concentration (CCC).

The bubble sizer sampling tube tip was positioned in the liquid phase, outside the turbulent region, to prevent the collection of froth bubbles and to allow gas hold-up measurements to be conducted under quiescent conditions. The sampling location remained constant within each unit throughout the test program.

The bubble viewer and its associated water reservoir were filled with frother solution at the same concentration as that in the cell to prevent dilution during bubble sampling. In the laboratory and pilot units, the cell overflow was recirculated to maintain the frother concentration throughout the tests. Overflow recirculation was not possible in the industrial unit because of limitations of the existing test arrangement. Thus, frother concentration control differed between the laboratory/pilot and industrial measurements. Fig. 2 shows the experimental setup. Each unit is equipped with pressure transmitters on the Blast Tube feed and air lines.

Blast Tube feed pressure, air pressure, feed flow rate, and air flow rate were continuously monitored and recorded during each test. Bubble size and gas hold-up were evaluated under the different operating conditions investigated at each scale. Gas hold-up was measured three times over 5 min at each operating condition, and the arithmetic mean of the three values was used in the subsequent analysis. The standard deviation of the repeated measurements was also calculated to assess measurement repeatability.

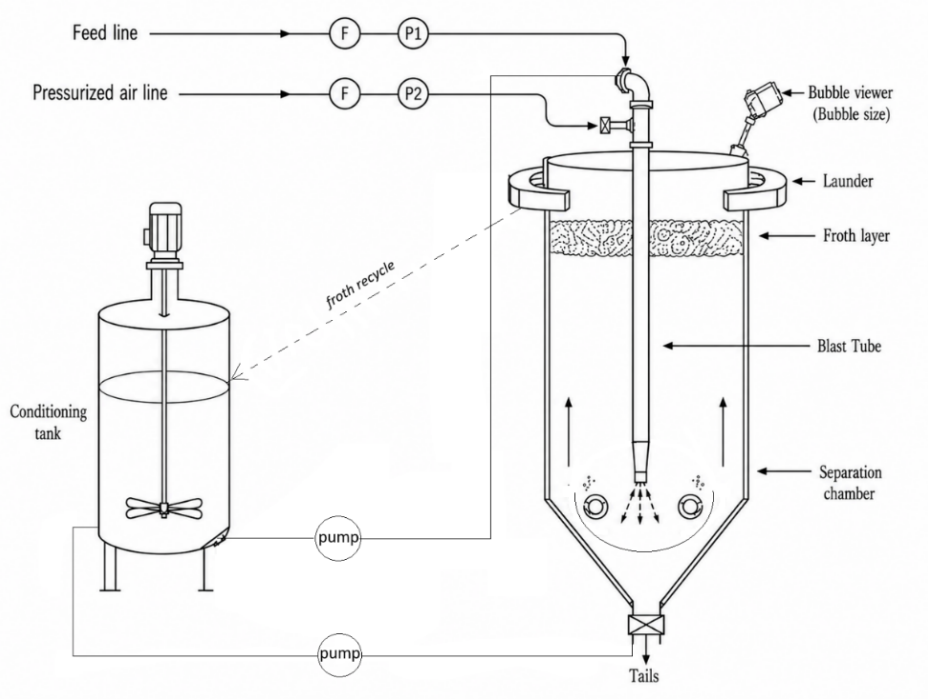

Fig. 2. Schematic diagram of experimental setup

3. Results and discussion

3.1. Effect of pressure and jet velocity on bubble size distribution

For comparison across laboratory, pilot and industrial units, the operating conditions were kept as close as practicable, including frother concentration, air-to-pulp ratio, pressure, jet velocity and geometric design ratios. Exact pressure matching was not possible because the available nozzle sizes in the laboratory and pilot units were not proportionally equivalent in diameter to those used in the industrial configuration. These feed and air pressure differences also caused variations in jet velocity. To assess whether this affected bubble size distribution, bubble size was measured at different pressure conditions within the same unit while all other operating parameters were maintained constant. Pressure was varied by changing both the top and bottom nozzle diameters of the Concorde Cell Pilot by 1 mm. Measured and calculated superficial gas velocities followed the same general trend but differed as J_g increased (Fig. 3). Calculated J_g was therefore used throughout this study.

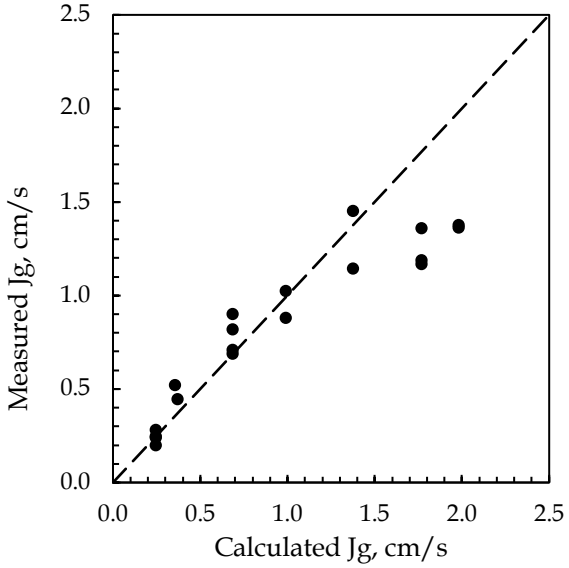

Fig. 3. Correlation of measured and calculated superficial gas velocities

Two nozzle configurations were used to establish the low- and high-pressure operating conditions. For each nozzle configuration, the nozzle remained unchanged while the air flow rate was varied to obtain the desired range of superficial gas velocities. The nozzle configuration was changed only after completion of the full J_g test series.

The cumulative bubble volume distribution obtained from each test was fitted to the Rosin – Rammler equation (Biswal et al., 1994) given as Eq. (1):

$$Q(d) = 100\left\{1 - \exp\left[-\left(\frac{d}{dc}\right)^n\right]\right\} \quad (1)$$

where d is the bubble diameter, d_c is the characteristic bubble diameter, and n is the distribution parameter.

Bubble size distributions are presented as cumulative volume fractions so that both fine and large bubble populations are represented in terms of their contribution to gas volume. This form is commonly used when discussing gas dispersion, where bubble volume and interfacial area are more relevant than bubble number alone (Finch et al., 2000). Fig. 4 shows the corresponding cumulative distributions as a function of bubble diameter for different superficial gas velocities. As J_g increased, the distributions shifted towards larger diameters and became broader, reflecting a greater contribution of coarse bubbles. Comparable increases in bubble size with gas rate have been reported in other flotation systems (Gorain et al., 1997; Schwarz and Alexander, 2006).

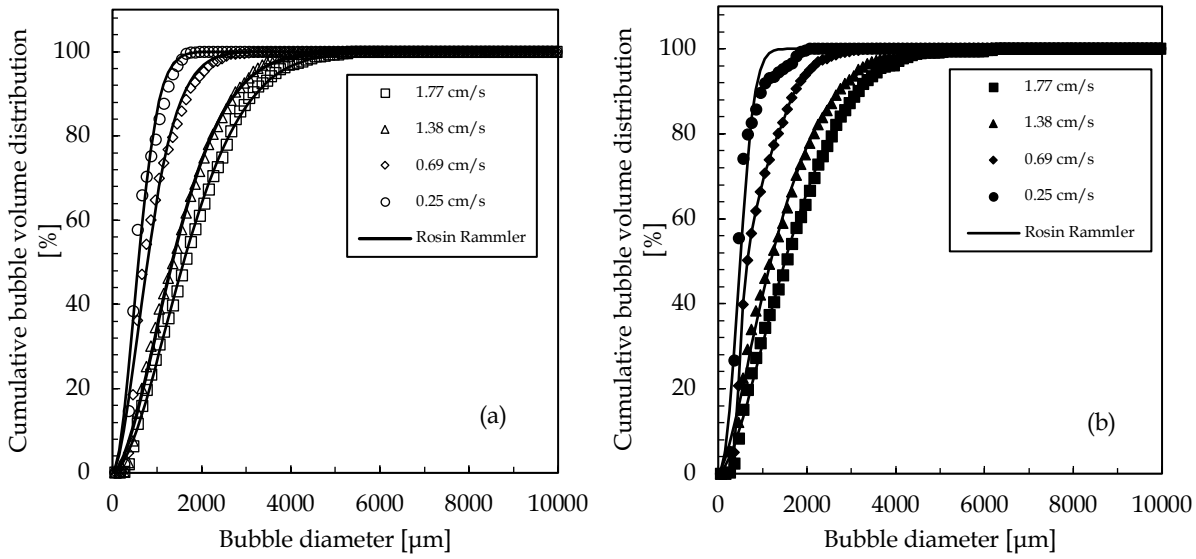

Fig. 4. Concorde Cell Pilot bubble size distributions at frother concentrations above the critical coalescence concentration (CCC) as a function of J_g: (a) small nozzle pair at high pressure (b) small nozzle pair at low pressure

Table 2 summarizes the characteristic bubble diameter (d_c) obtained from the Rosin–Rammler fits. The fitted $d_c$values increased consistently with J_g for both nozzle configurations, confirming the progressive shift of the cumulative bubble size distributions towards larger diameters with increasing gas rate. The differences in d_c between the two nozzle configurations were comparatively small, indicating that J_g had a greater influence on the cumulative bubble size distribution than the pressure and jet-velocity differences investigated.

Table 2. Rosin Rammler fitting parameter, d_c

J_g (cm/s)	d_c (µm) (high pressure /high jet velocity)	d_c (µm) (low pressure/low jet velocity)
1.77	1978	1892
1.38	1672	1528
0.69	971	951
0.25	699	577

The bubble volume distributions were also fitted using the upper-limit distribution proposed by Mugele and Evans (1951), following the approach of Grau and Heiskanen (2005), who showed that this model satisfactorily represented bubble size distributions measured in laboratory-scale flotation cells. The equation is presented in Eq. (2):

$$\frac{dV}{db} = \frac{\delta}{\sqrt{\pi}} \frac{d_{b\,max}}{d_b(d_{b\,max} - d_b)} exp\left\{-\delta^2 \left[\ln \frac{a\,d_b}{d_{b\,max} - d_b}\right]\right\}^2 \quad (2)$$

where d_b is the bubble diameter, $d_{b\,max}$ is the upper limit of bubble diameter, and V is the bubble volume fraction. The coefficient a determines the distribution position along the bubble-size axis, while δ describes its width; larger values of δ correspond to a narrower distribution.

Fig. 5 shows the differential bubble volume distributions obtained at high and low pressure over the J_g range of 0.25–1.77 cm/s. Increasing J_g reduced the height of the distribution maximum and increased the contribution of larger bubbles, resulting in a broader bubble population at higher superficial gas velocities. The observed difference cannot be attributed to pressure alone because pressure and nozzle jet velocity changed simultaneously.

The effect of pressure was most pronounced at a J_g of 0.25 cm/s, where the distribution maximum was greater under the lower-pressure condition, while the diameter at the distribution peak remained similar. This may be associated with increased bubble break-up under the local shear expected at higher jet velocity (Hinze, 1955). At superficial gas velocities of 0.69 and 1.38 cm/s, the difference between the two pressure conditions became less evident. In this range, bubble size reflects the combined effect of gas rate and local hydrodynamics (Dahlke et al., 2005; Nesset et al., 2006). At the highest J_g of 1.77 cm/s, the distributions were similar, with only minor changes in peak position, suggesting that bubble size was governed primarily by gas rate with reduced sensitivity to pressure. The high pressure/ high jet velocity condition shifted the distribution towards smaller diameters and reduced the large bubble fraction, whereas increasing J_g produced larger bubbles and broader distributions; within the investigated range, J_g had a more pronounced effect on the distribution width and large-bubble fraction than the combined pressure and jet velocity differences examined in the pilot unit.

Table 3 summarizes the Upper-Limit fitting parameter a, which describes the position of the differential bubble size distribution along the bubble diameter axis. Unlike the Rosin–Rammler characteristic diameter (d_c), which is obtained from the cumulative bubble volume distribution, the Upper-Limit parameter a describes the position of the differential bubble size distribution along the bubble diameter axis. Consequently, the two parameters characterize different aspects of the bubble population and should not be interpreted as directly comparable. The lower a values obtained under the high-pressure (small-nozzle) configuration indicate that the differential bubble size distribution was shifted towards smaller bubble diameters, consistent with the distributions shown in Fig. 5. This behaviour may be associated with differences in the local hydrodynamic conditions between the two nozzle configurations, potentially affecting local energy dissipation and bubble break-up (Prince and Blanch, 1990).

Both operating conditions were evaluated at frother concentrations above the critical coalescence concentration; therefore, differences in the fitted distributions are attributed primarily to changes in the hydrodynamic conditions rather than variations in bubble coalescence caused by frother concentration (Kowalczuk, 2013).

3.2 Industrial Concorde Cell bubble size distributions

Fig. 6 presents the bubble volume distribution measured in the industrial Concorde Cell at superficial gas velocities from 0.35 to 2.54 cm/s. As observed in the pilot cell, the cumulative curves shifted towards larger bubble diameters with increasing J_g. The industrial and pilot units produced distributions with peaks in comparable bubble-size ranges, generally around 400–600 μm. The narrowest distribution was obtained at the lowest superficial gas velocities. Although the exact J_g values differed because of the tank cross-sectional areas, both units showed a transition from a narrow, fine-bubble population at low gas velocity to a broader distribution with more large bubbles as J_g increased. The gas-rate effect was most pronounced at low and intermediate J_g, and became less significant at higher values. Increases in

bubble size with gas rate have also been reported from measurements in full-scale flotation cells (Hernandez-Aguilar et al., 2002).

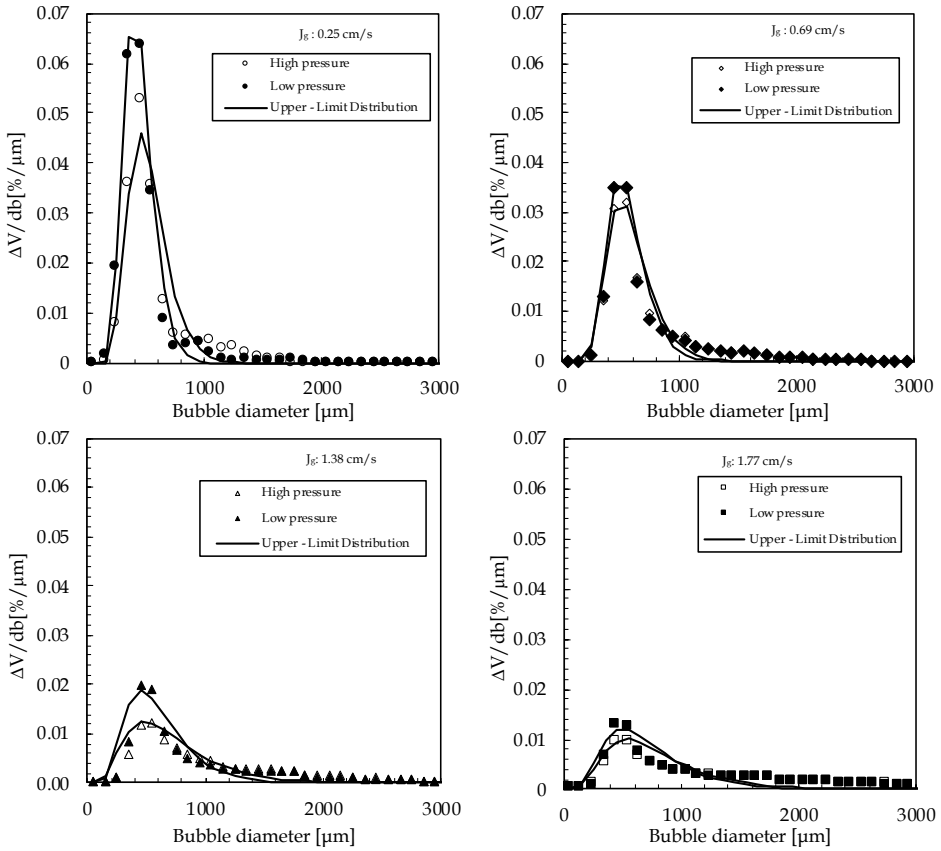

Fig. 5. Differential bubble size distributions as a function of J_g under low- and high-pressure conditions

Table 3. Upper limit fitting parameter, a

J_g (cm/s)	Small Nozzle (high pressure)	Large Nozzle (low pressure)
0.25	20.2	22.4
0.69	16.9	20.0
1.38	11.9	17.0
1.77	9.0	13.0

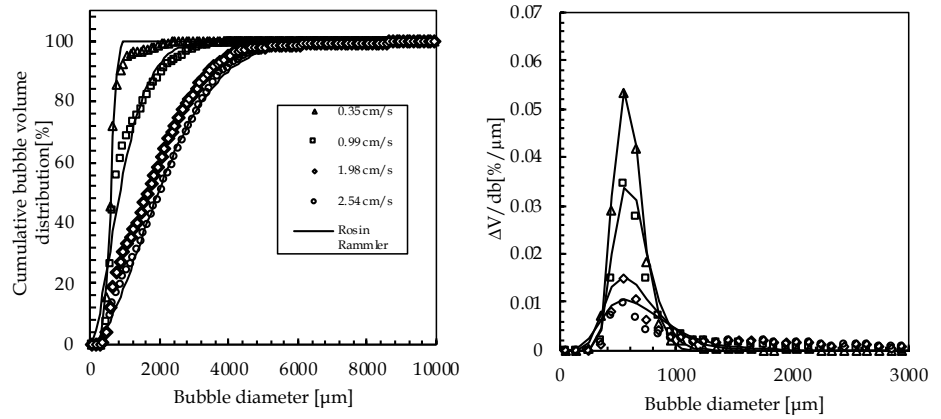

Fig. 6. Concorde Cell Industrial bubble size distributions at frother concentrations above the critical coalescence concentration (CCC) as a function of J_g

3.3 Gas dispersion comparison

Fig. 7 compares the differential bubble volume distributions obtained in the pilot and industrial Concorde Cells at corresponding low and high superficial gas velocities. Because the J_g values were not identical between the two units, the comparison represents similar gas-rate regions rather than directly matched operating conditions. The measurements agree well with the trends described above. At the lower J_g condition, the industrial distribution showed a clear shift in the peak toward larger bubble diameters, from approximately 450–500 µm in the pilot unit to 550–600 µm in the industrial unit. This difference is most likely associated with the slightly higher J_g in the industrial cell, 0.35 cm/s compared with 0.25 cm/s in the pilot cell, rather than an inherent scale effect. Kim and Park (2024) similarly observed an increase in bubble size with gas velocity in a flotation column and related this behaviour to increased collision and coalescence. The comparison of the complete distributions is important because similar mean bubble diameter may arise from bubble populations having different distribution widths and coarse-bubble fractions, as discussed by Vazirizadeh et al. (2016).

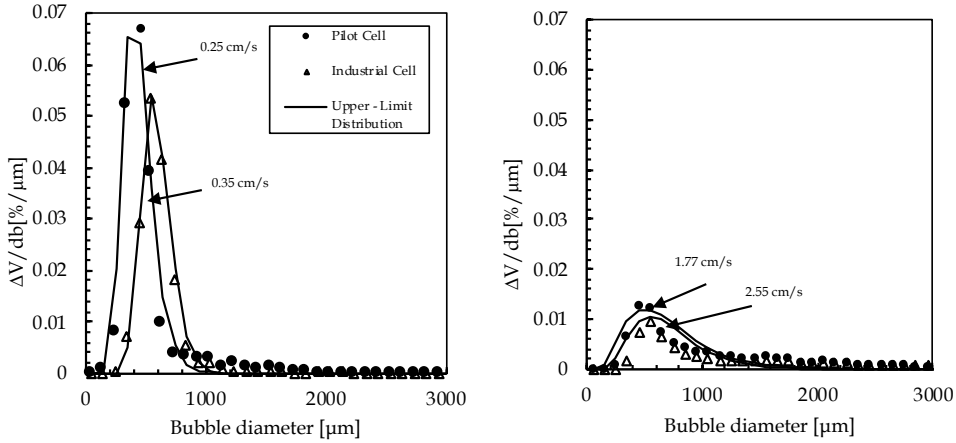

Fig. 7. Concorde Industrial versus Pilot Cell bubble size distribution comparison above CCC as a function of J_g

The Sauter mean diameter increased approximately linearly with J_g at all three scales (Fig. 8). This trend agrees with laboratory flotation cell measurements by Femenias et al. (2022), who reported increasing d_{32} with J_g. For bubble size measurements, three repeated measurements at the same operating condition gave d_{32} values of 0.566, 0.515, and 0.476 mm, corresponding to a mean d_{32} of 0.519 ± 0.045 mm. The pilot- and industrial-scale measurements showed close agreement over the common range of J_g, whereas the laboratory data followed a similar trend but gave slightly larger d_{32} values at the lower gas velocities. This offset may be influenced by the use of an alcohol based frother in the laboratory unit, because bubble size is sensitive to frother type and chemical characteristics (O'Connor,

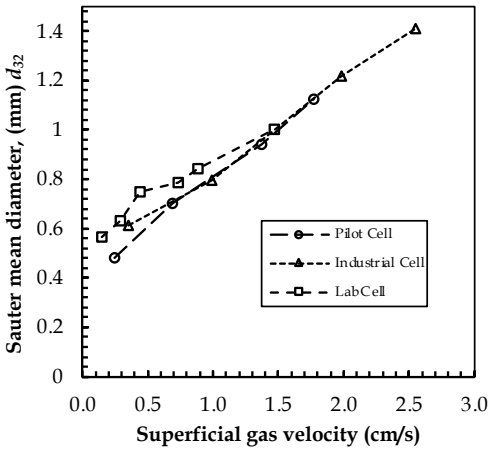

Fig. 8. Sauter mean bubble diameter as a function of J_g in the laboratory, pilot and industrial Concorde Cells at frother concentrations above the CCC

Randall and Goodall, 1990), in addition to scale-related effects. Therefore, the laboratory-to-pilot comparison should be interpreted with caution. Overall, the close agreement between the pilot and industrial scale measurements, obtained using the same frother type, provides stronger evidence that the d_{32} – J_g relationship was maintained across these scales.

Bubble surface area flux increased with gas hold-up in both the pilot and industrial units Fig. 9(a) The two datasets followed nearly the same trend over the common range, while industrial measurements extended to higher gas hold-up and bubble surface area flux. Compared with TankCell 1, e300 and e500 data reported by Grau et al. (2014), the Concorde Cell obtained higher gas hold-up. In the TankCell e500, gas hold-up increased from approximately 4% at a local J_g of 0.2 cm/s to about 9–10% at J_g values approaching 1.0 cm/s. Over a similar range, the Concorde Cell produced gas hold-ups of approximately 4–7% at J_g of 0.25 - 0.35 cm/s and 10–12% at J_g of 0.69 - 0.99 cm/s. This comparison is made at comparable J_g values; however, the two systems differ in air-to-pulp ratio, cell geometry, and gas dispersion mechanism, and therefore the results are not directly comparable. The repeatability of the gas hold-up measurements was assessed from three repeated measurements at each operating condition. The corresponding standard deviations were 0.81, 0.70, 5.19, and 4.76 percentage points at J_g values of 0.37, 0.99, 1.98, and 2.55 cm/s, respectively. At higher gas rates, the Concorde gas hold-up increased further, reaching approximately 26–35%. The higher gas hold-up means that a larger fraction of the cell volume was occupied by dispersed gas, which is consistent with the high-intensity pneumatic contacting conditions in the Concorde Cell (Kupka et al., 2023; Mattsson et al., 2025). High gas hold-up alone, however, should not be taken as a direct measure of improved metallurgical performance.

The laboratory, pilot, and industrial data showed close correspondence in the variation of S_b with J_g demonstrating consistent gas dispersion behaviour across scale (Fig. 9(b)). This agreement shows that the combined effect of gas rate and bubble size was maintained from laboratory to industrial scale. Massinaei et al. (2009) similarly compared pilot and industrial flotation columns and found that the collection-zone rate constant was related to gas hold-up and bubble surface area flux rather than to J_g or bubble size separately. The preservation of these gas-dispersion relationships supports scale-up of the pulp zone hydrodynamic conditions in the Concorde Cell.

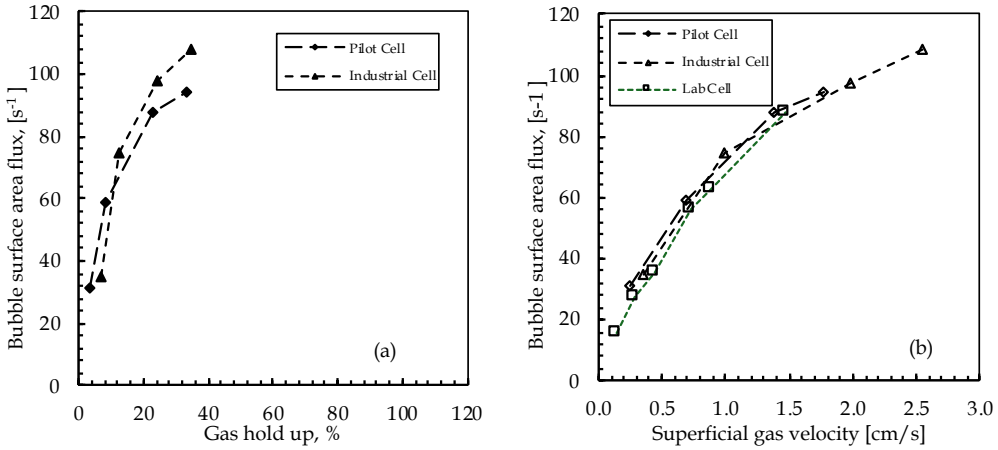

Fig. 9. Bubble surface area flux as a function of (a) gas hold-up in the pilot and industrial Concorde Cells and (b) J_g in the laboratory, pilot, and industrial Concorde Cells

4. Conclusions

This study investigated the gas-dispersion characteristics of the Concorde Cell in two-phase systems at laboratory, pilot, and industrial scales. The main conclusions are: Increasing J_g shifted the bubble volume distributions towards larger diameters and increased the contribution of large bubbles. Consequently, the distributions became broader as J_g increased.

- The high-pressure/high-jet-velocity condition produced somewhat smaller bubbles and a lower large-bubble fraction, particularly at the lowest J_g. This difference became less evident as the gas rate increased. Since pressure and nozzle jet velocity varied simultaneously, their individual contributions could not be separated.

- The Rosin–Rammler and Upper-Limit distribution models provided complementary descriptions of the bubble size distributions. While the Rosin–Rammler characteristic diameter (d_c) represented the cumulative bubble population, the Upper-Limit parameter (a) quantified the position of the differential distribution, confirming that the high-pressure operating condition shifted the bubble population towards finer diameters without altering the overall trends governed by J_g.
- J_g had a greater influence on bubble size and distribution width than the pressure and jet-velocity differences investigated in the pilot unit.
- The pilot and industrial units produced comparable bubble volume distributions. The shift of the industrial distribution towards a larger peak diameter at the lowest gas-rate condition was consistent with its slightly higher J_g rather than with a distinct scale effect.
- The Sauter mean bubble diameter increased with J_g at all three scales. The pilot and industrial data overlapped over the common operating range, while the laboratory unit produced slightly larger bubbles at low J_g, attributed to the alcohol-based frother used in the laboratory tests.
- Gas hold-up and bubble surface area flux increased with gas rate. Gas hold-up reached approximately 26–35% at the highest pilot and industrial operating conditions, while bubble surface area flux exceeded 100 s^{-1} in the industrial unit.
- The variation of d_{32}, gas hold-up, and S_b with J_g was maintained from laboratory to industrial scale. The agreement among these gas-dispersion parameters supports direct scale-up of the pulp-zone gas-dispersion conditions of the Concorde Cell over the investigated operating range.

The conclusions are restricted to two-phase operation at frother concentrations above the critical coalescence concentration. Metallurgical scale-up must additionally account for the effects of solids, particle loading, residence time, and froth transport.

Acknowledgments

The authors would like to thank Pedro Aquino for his contribution during his summer work in 2024 and Sevda Dilmaghani for her assistance with gas hold-up measurements in the pilot unit. The authors are also grateful to Ian Sherrell for his careful review of the manuscript and his valuable comments and suggestions, which helped improve its quality. The support provided by the personnel of the Metso Mineral Processing Laboratory and Pilot Plant at the Pori Research Center during the experimental work is gratefully acknowledged. The authors also thank Boliden Kevitsa for their collaboration and support throughout the study. A part of the results reported in this paper were presented at XX Balkan Mineral Processing Congress BMPC 2026 entitled "Gas dispersion characteristics of the Concorde Cell™".

References

AHMADI, R., KHODADADI, D.A., ABDOLLAHY, M., FAN, M., 2014. *Nano-microbubble flotation of fine and ultrafine chalcopyrite particles.* International Journal of Mining Science and Technology, 24(4), 559–566.

BISWAL, S.K., REDDY, P.S.R., BHAUMIK, S.K., 1994. *Bubble size distribution in a flotation column.* The Canadian Journal of Chemical Engineering, 72(1), 148-152.

BURSTEIN, M., FILIPPOV, L., 2010. *Scale-up of flotation processes.* Computational Science Research Center Report, San Diego State University.

CALVO, G. and VALERO, A., 2022. *Strategic mineral resources: Availability and future estimations for the renewable energy sector*. Environmental Development, 41, 100640.

DAHLKE, R., GOMEZ, C.O. and FINCH, J.A., 2005. *Operating range of a flotation cell determined from gas holdup versus gas rate.* Minerals Engineering, 18(9), 977–980.

DAI, Z., FORNASİERO, D. and RALSTON, J., 1999. *Particle–bubble attachment in mineral flotation*. Journal of Colloid and Interface Science, 217(1), 70–76.

FARROKHPAY, S., FILIPPOV, L. and FORNASIERO, D., 2021. *Flotation of fine particles: A review*. Mineral Processing and Extractive Metallurgy Review, 42(7), 473-483.

FEMENIAS, F., MALDONADO, M., MIRANDA, N., GUTIERREZ, L., 2022. *Flotation performance and gas dispersion properties in a laboratory flotation cell*. Minerals, 12, 1351.

FINCH, J.A., XIAO, J., HARDIE, C., GOMEZ, C.O., 2000. *Gas dispersion properties: bubble surface area flux and gas holdup.* Minerals Engineering, 13(4), 365-372.

GOMEZ, C.O., FINCH, J.A., 2007. *Gas dispersion measurements in flotation cells*. International Journal of Mineral Processing, 84 (1–4), 51–58.

GORAIN, B. K.1997. *The effect of bubble surface area flux on the kinetics of flotation and its relevance to scale-up*. PhD Thesis.

GORAIN, B.K., FRANZIDIS, J.P., MANLAPIG, E.V., 1997. *Studies on impeller type, impeller speed and air flow rate in an industrial scale flotation cell: Part 4. Effect of bubble surface area flux on flotation performance*. Minerals Engineering, 10, 367–379.

GRAU, R.A., HEISKANEN, K., 2005. *Bubble size distribution in laboratory scale flotation cells*. Minerals Engineering, 18(12), 1164–1172.

HERNANDEZ, J.R., 2002. *A technique for the direct measurement of bubble size distributions in industrial flotation cells.* In Annual Meeting of the January (Vol. 22, p. 24).

HERNANDEZ-AGUILAR, J.R., GOMEZ, C.O., FINCH, J.A., 2002. *A technique for the direct measurement of bubble size distributions in industrial flotation cells*. In: Proceedings of the 34th Annual Meeting of the Canadian Mineral Processors, Ottawa, Canada, 22–24 January 2002, pp. 389–402.

HINZE, J.O., 1955. *Fundamentals of the hydrodynamic mechanism of splitting in dispersion processes*. AIChE Journal, 1(3), 289–295.

JAMESON, G.J., 2010. *Advances in fine and coarse particle flotation*. Canadian Metallurgical Quarterly, 49(4), 325–330.

KIM, H.S., PARK, C.-H., 2024. *Estimation of bubble size and gas dispersion property in column flotation*. Separations, 11(12), 331.

KLIMPEL, R.R., 1984. *Use of chemical reagents in flotation*. Chemical Engineering (New York, NY), 91(18), 75-79.

KOWALCZUK, P.B., 2013. *Determination of critical coalescence concentration and bubble size for surfactants used as flotation frothers*. Industrial & Engineering Chemistry Research, 52, 11752–11757.

KUPKA, N., SUHONEN, J., TUNÇ, B., YÁÑEZ, A., RINNE, A., 2023**.** *Metallurgical performance of the Concorde Cell™ at industrial scale*. Flotation '23, Cape Town, South Africa.

MASSINAEI, M., KOLAHDOOZAN, M., NOAPARAST, M., OLIAZADEH, M., YIANATOS, J., SHAMSADINI, R., YARAHMADI, M., 2009. *Hydrodynamic and kinetic characterization of industrial columns in rougher circuit*. Minerals Engineering, 22(4), 357–365.

MATTSSON, T., KELA, H., MUSUKU, B., KASALA, M., YÁÑEZ, A., 2025**.** *Industrial scale performance of Concorde Cell™ technology at Kevitsa Cu–Ni–PGM concentrator*. Flotation '25, Cape Town, South Africa.

MUGELE, R.A., EVANS, H.D., 1951. *Droplet size distribution in sprays*. Industrial & Engineering Chemistry, 43(6), 1317–1324.

NESSET, J.E., HERNANDEZ-AGUILAR, J.R., ACUNA, C., GOMEZ, C.O. AND FINCH, J.A., 2006. *Some gas dispersion characteristics of mechanical flotation machines.* Minerals Engineering, 19(6–8), 807–815.

O'CONNOR, C.T., RANDALL, E.W., GOODALL, C.M., 1990. *Measurement of the effects of physical and chemical variables on bubble size*. International Journal of Mineral Processing, 28, 139–149.

PEASE, J., CURRY, D.C. and YOUNG, M., 2006. *Designing flotation circuits for high fines recovery*. Minerals Engineering, 19(6–8), 831–840.

PIXACT, 2026. *Bubbles and foams: Pixact Bubble Monitoring*. Pixact Ltd., Tampere, Finland. Accessed 10 June 2026.

PRINCE, M.J., and BLANCH, H.W., 1990. *Bubble coalescence and break-up in air-sparged bubble columns.* AIChE Journal, 36(10), 1485-1499.

SAEED, M., DE SOUZA, C.V., CHIPAKWE, V., CHELGANI, S.C., 2022. *Influence of hydrodynamic variables on scaling up of mechanical flotation cells.* Arabian Journal of Geosciences, 15, 1 - 14

SCHUBERT, H., 2008. *On the optimization of hydrodynamics in fine particle flotation.* Minerals Engineering, 21(12–14), 930–936.

SCHWARZ, S., and ALEXANDER, D., 2006. *Gas dispersion measurements in industrial flotation cells.* Minerals Engineering, 19(6–8), 554–560.

VAZIRIZADEH, A., BOUCHARD, J., CHEN, Y., 2016. *Effect of particles on bubble size distribution and gas hold-up in column flotation.* International Journal of Mineral Processing, 157, 163–173.

YOON, R.H., LUTTRELL, G.H., 1989. *The effect of bubble size on fine particle flotation.* Mineral Processing and Extractive Metallurgy Review, 5(1–4), 101–122.